Determination of the 3D structures …

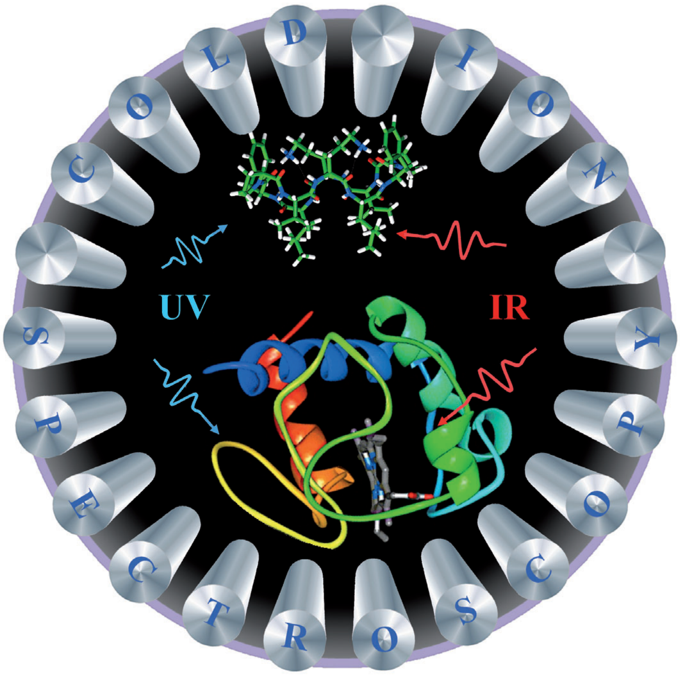

… of large molecules challenges spectroscopy to perform better. In their Communication on page 6002 ff. O. V. Boyarkin et al. use IR–UV double-resonance cold-ion spectroscopy for conformational assignment of the electronic spectra of a protonated decapeptide and for measurements of absolute absorption cross-sections of vibrational transitions in this species. The limitations of the IR–UV double-resonance approach are illustrated by measuring the gas-phase IR spectrum of a cold, protonated intact protein.

Controlled Release

In their Communication on page 5956 ff. P. Matteini et al. show how nanocomposite films can be used to “stamp” biological tissues and cells. The driving force is photothermal conversion from gold nanoparticles in the film.

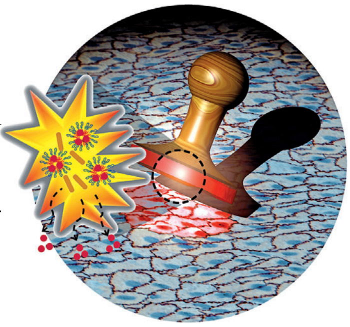

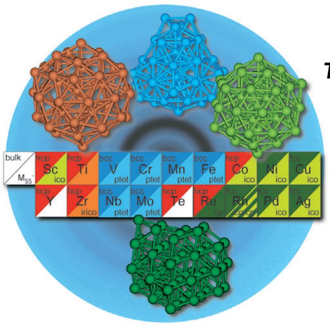

Transition-Metal Clusters

In their Communication on page 6102 ff., D. Schooss et al. use gas-phase electron diffraction of 55-atom clusters to show a correlation between the cluster structure type and the bulk structure.

Polycyclic Hydrocarbons

In their Communication on page 6076 ff., Y. Tobe et al. present the first example of a *meta*-quinodimethane embedded in an indenofluorene framework. Despite its small conjugation space, the compound exhibits a very-low-energy light-absorption band.

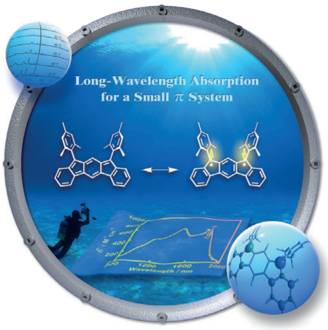

How to contact us:

Editorial Office:
E-mail: angewandte@wiley-vch.de
Fax: (+49) 6201–606-331
Telephone: (+49) 6201–606-315

Reprints, E-Prints, Posters, Calendars:
Carmen Leitner
E-mail: chem-reprints@wiley-vch.de
Fax: (+49) 6201–606-331
Telephone: (+49) 6201–606-327

Copyright Permission:
Bettina Loycke
E-mail: rights-and-licences@wiley-vch.de
Fax: (+49) 6201–606-332
Telephone: (+49) 6201–606-280

Online Open:
Margitta Schmitt, Carmen Leitner
E-mail: angewandte@wiley-vch.de
Fax: (+49) 6201–606-331
Telephone: (+49) 6201–606-315

Subscriptions:
www.wileycustomerhelp.com
Fax: (+49) 6201–606-184
Telephone: 0800 1800536 (Germany only)
+44(0) 1865476721 (all other countries)

Advertising:
Marion Schulz
E-mail: mschulz@wiley-vch.de
jspiess@wiley-vch.de
Fax: (+49) 6201–606-550
Telephone: (+49) 6201–606-565

Courier Services:
Boschstrasse 12, 69469 Weinheim

Regular Mail:
Postfach 101161, 69451 Weinheim

Angewandte Chemie International Edition is a journal of the Gesellschaft Deutscher Chemiker (GDCh), the largest chemistry-related scientific society in continental Europe. Information on the various activities and services of the GDCh, for example, cheaper subscription to *Angewandte Chemie International Edition*, as well as applications for membership can be found at **www.gdch.de** or can be requested from GDCh, Postfach 900440, D-60444 Frankfurt am Main, Germany.

GDCh
GESELLSCHAFT
DEUTSCHER CHEMIKER

Service

Author Profile

"My favorite book is Doktor Faustus. The natural talent I would like to be gifted with being able to improvise on the piano. …"
This and more about Christian Griesinger can be found on page 5912.

Books

Highlights

Carbocyclization

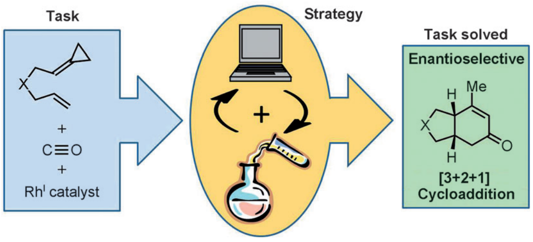

In silico veritas? Maybe not the whole truth, but very helpful suggestions and guidelines for the experimental work can be deduced from computational studies on Rh-catalyzed [3+2+1] cycloaddition reactions for the construction of *cis*-fused bicyclohexenones from alkylidenecyclopropanes and carbon monoxide.

Computational Studies and Experimental Results—An Example of Excellent Teamwork in Studying Carbocyclization

C—C and C—N Coupling

M. Majek,
A. Jacobi von Wangelin* ____ 5919–5921

Ambient-Light-Mediated Copper-Catalyzed C—C and C—N Bond Formation

Bringing to light: The rediscovery of visible light as an abundant energy source for organic reactions has most recently brought copper-catalyzed coupling reactions to the center of attention. This Highlight summarizes the most significant advancements in the field of C—C and C—N coupling reactions in which covalent copper–substrate complexes are photoactivated.

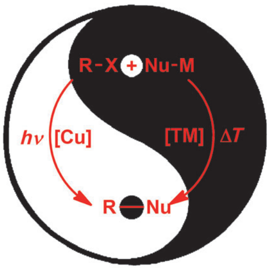

Correspondence

Chemical Bonding

G. Frenking,* M. Hermann _ 5922–5925

Critical Comments on “One Molecule, Two Atoms, Three Views, Four Bonds?”

The arguments that are given in the original trialogue in favor of a quadruply bonded C_2, in which the bond is claimed to be stronger than that in HC≡CH, are judged invalid by the authors of this Correspondence. They also disagree with some statements about the stability of molecules and the virtue of chemical research beyond synthetic chemistry.

Chemical Bonding

D. Danovich, S. Shaik,* H. S. Rzepa,*
R. Hoffmann* ____________ 5926–5928

A Response to the Critical Comments on “One Molecule, Two Atoms, Three Views, Four Bonds?”

The criticism expressed by Frenking and Hermann on the notion of quadruple bonding in C_2 is answered using hard facts. Both experimental and computational data gauge the strength of the fourth bond as 16 kcal mol^{-1}. The authors agree that chemical research goes profitably beyond “synthetic” chemistry.

Minireviews

Click Chemistry

M. A. Tasdelen,* Y. Yagci* _ 5930–5938

Light-Induced Click Reactions

Shine a light: Owing to their ease of implementation and the availability of inexpensive light sources, light-induced click reactions (see picture) have become a powerful methodology for the synthesis of materials and the modification of biomaterials. Fundamental aspects of these reactions and their application in surface and materials science, as well as their potential in the study of biomolecular systems are highlighted.

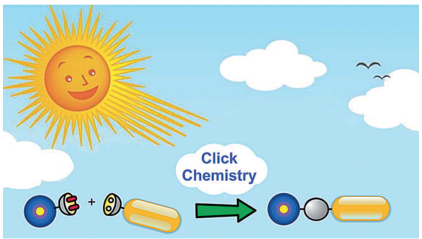

For the USA and Canada: ANGEWANDTE CHEMIE International Edition (ISSN 1433-7851) is published weekly by Wiley-VCH, PO Box 191161, 69451 Weinheim, Germany. Air freight and mailing in the USA by Publications Expediting Inc., 200 Meacham Ave., Elmont, NY 11003. Periodicals postage paid at Jamaica, NY 11431. US POSTMASTER: send address changes to *Angewandte Chemie*, Journal Customer Services, John Wiley & Sons Inc., 350 Main St., Malden, MA 02148-5020. Annual subscription price for institutions: US$ 11.738/10.206 (valid for print and electronic / print or electronic delivery); for individuals who are personal members of a national chemical society prices are available on request. Postage and handling charges included. All prices are subject to local VAT/sales tax.

Reviews

Spectroscopic Methods

Getting to the point: Tip-enhanced Raman spectroscopy (TERS) combines the chemical information of Raman spectroscopy experiments with a high signal enhancement and high spatial resolution. The current status of the technique is described together with the shortcomings and pitfalls that have to be considered for spectroscopic imaging by TERS.

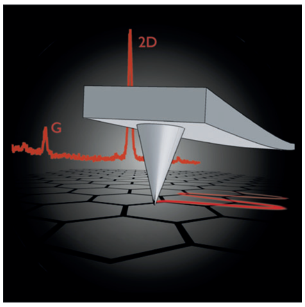

Communications

Controlled Release

Frontispiece

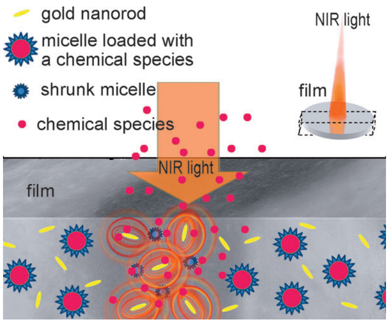

Illuminating films of a porous chitosan matrix containing gold nanorods and thermosensitive micelles loaded with a chemical stimulates local photothermal conversion of the gold nanorods. The heat produced activates the ejection of the chemical from the micelles (see scheme), and causes the transient permeabilization of adjacent cell membranes, resulting in a selective cellular uptake of the released chemical with control over spatiotemporal parameters and dosage.

Synthetic Methods

A 100 % atom-efficient synthesis of ketones from electron-deficient internal olefins was achieved using O_2 as a "green" oxidant (see scheme, DMA = *N*,*N*-dimethylacetamide, EWG = electron-withdrawing group). Various electron-deficient olefins were oxidized to the corresponding ketones with over 99 % selectivity and without the formation of olefin isomers or their oxidized products.

Ultrabright Nanoparticles

Stars that shine bright: A high local dye concentration in doped silica-based core–shell nanoparticles causes self-quenching and spectral broadening (top images). This phenomenon jeopardizes the potential advantages of heavily doped systems. Förster resonance energy transfer (FRET) to an acceptor co-included in the silica led to ultrabright nanoparticles (bottom images) with a preselected narrow-band emission and a pseudo-Stokes shift of 129 nm.

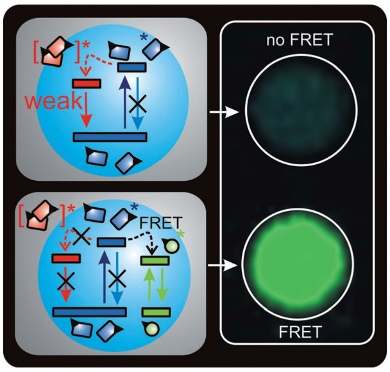

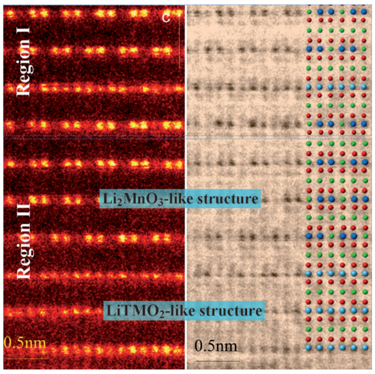

About phase: The coexistence of rhombohedral $LiTMO_2$ (TM = Ni, Co, or Mn) and monoclinic Li_2MnO_3-like structures inside $Li_{1.2}Mn_{0.567}Ni_{0.166}Co_{0.067}O_2$ is revealed directly at atomic resolution. The hetero-interface along the $[001]_{rh}/[103]_{mon}$ zone axis direction is demonstrated, indicating the two-phase nature of these lithium-rich cathode materials (green Li, blue Mn, red O, cyan TM).

Electron Microscopy

H. J. Yu, R. Ishikawa, Y. G. So, N. Shibata, T. Kudo, H. S. Zhou,* Y. Ikuhara* ______ **5969 – 5973**

Direct Atomic-Resolution Observation of Two Phases in the $Li_{1.2}Mn_{0.567}Ni_{0.166}Co_{0.067}O_2$ Cathode Material for Lithium-Ion Batteries

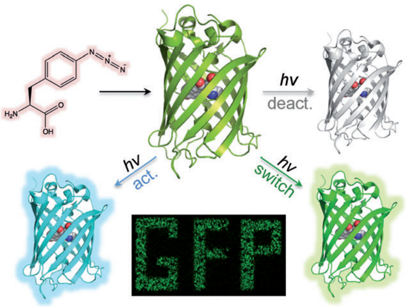

Expanding the genetic code opens new avenues to modulate protein function in real time. By genetically incorporating photoreactive phenyl azide, the fluorescent properties of green fluorescent protein (GFP) can be modulated by light. Depending on the residue in GFP programmed to incorporate the phenyl azide, different effects on function and photochemical pathways are observed.

Protein Photocontrol

S. C. Reddington, P. J. Rizkallah, P. D. Watson, R. Pearson, E. M. Tippmann,* D. D. Jones* ______ **5974 – 5977**

Different Photochemical Events of a Genetically Encoded Phenyl Azide Define and Modulate GFP Fluorescence

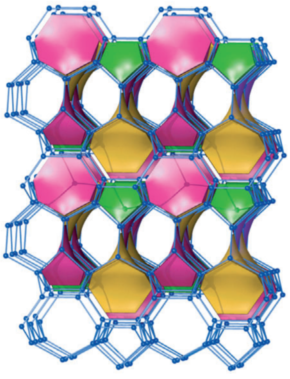

Silicon swallows up boron: The novel open tetrahedral framework structure (OTF) of the Zintl phase $LiBSi_2$ was made by applying high pressure to a mixture of LiB and elemental silicon. The compound represents a new topology in the B-Si net (called **tum**), which hosts Li atoms in the channels (see picture). $LiBSi_2$ is the first example where B and Si atoms form an ordered common framework structure with B engaged exclusively in heteronuclear B—Si contacts.

Zintl Phases

M. Zeilinger, L. van Wüllen, D. Benson, V. F. Kranak, S. Konar, T. F. Fässler,* U. Häussermann* ______ **5978 – 5982**

$LiBSi_2$: A Tetrahedral Semiconductor Framework from Boron and Silicon Atoms Bearing Lithium Atoms in the Channels

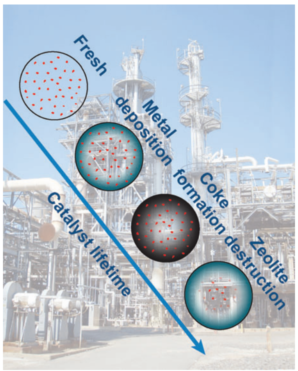

Fluid catalytic cracking (FCC) is the main conversion process used in oil refineries. An X-ray microscopy method is used to show that metal poisoning and related structural changes in the zeolite active material lead to a non-uniform core–shell deactivation of FCC catalyst particles. The study links the detrimental effect of V and Ni poisoning with zeolite destruction and dealumination in a spatial manner within a single FCC catalyst particle.

Heterogeneous Catalysis

J. Ruiz-Martínez, A. M. Beale,* U. Deka, M. G. O'Brien, P. D. Quinn, J. F. W. Mosselmans, B. M. Weckhuysen* ______ **5983 – 5987**

Correlating Metal Poisoning with Zeolite Deactivation in an Individual Catalyst Particle by Chemical and Phase-Sensitive X-ray Microscopy

Photoresponsive Polymers

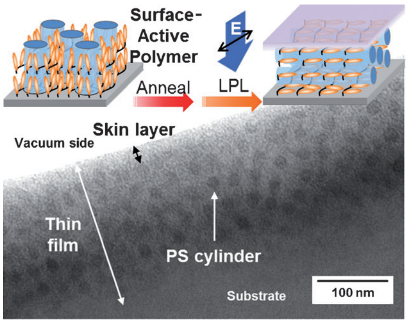

An orientational change from homeotropic to planar of liquid crystal (LC) mesogens and the microphase separation (MPS) domains is attained by the segregated skin layer at the free surface. This allows for an efficient in-plane photoalignment of the cylindrical domains. The surface segregation strategy is very simple and is therefore expected to open up new possibilities for the orientation control of various types of LC materials.

Carbocycles

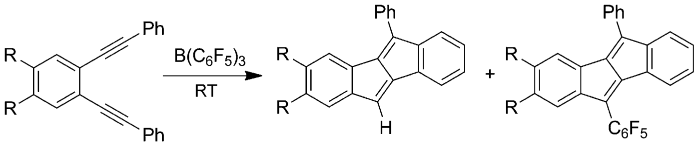

'Lene' and mean: The strong Lewis acid $B(C_6F_5)_3$ efficiently converts some bis(arylethynyl)benzenes into dibenzopentalenes through a series of Lewis acid induced cyclization reactions at room temperature. Thus the reaction has the potential to be useful in the synthesis of substituted dibenzopentalene derivatives which are difficult to make by conventional means.

Lithium Ion Battery

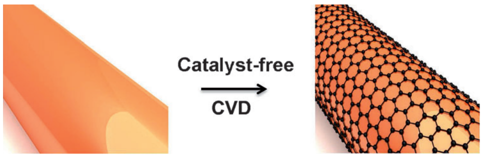

Direct growth of a single to a few layers of graphene on a germanium nanowire (Gr/Ge NW; see picture) was achieved by a metal-catalyst-free chemical vapor deposition (CVD) process. The Gr/Ge NW was used as anode in a lithium ion battery. This material has a specific capacity of 1059 mA h g^{-1} at 4.0 C, a long cycle life over 200 cycles, and a high capacity retention of 90%.

Structure Elucidation

Front Cover

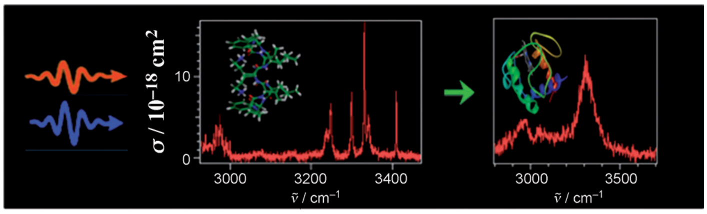

Spectroscopic fingerprint: Infrared–ultraviolet double resonance photodissociation is used for conformational assignment of the electronic spectra of a cold protonated decapeptide (see picture). A mechanism of the IR–UV depletion spectroscopy is proposed and a procedure of using it for measurements of absolute absorption cross-sections of vibrational transitions is elaborated.

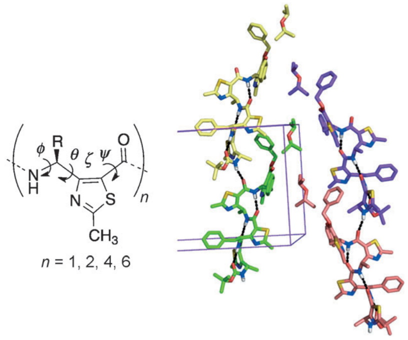

9-Helix: 4-Amino(methyl)-1,3-thiazole-5-carboxylic acids (ATCs) were synthesized as new γ-amino acid building blocks. The structures of various ATC oligomers were analyzed in solution by CD and NMR spectroscopy and in the solid state by X-ray crystallography. The ATC sequences adopted a well-defined 9-helix structure in the solid state and in aprotic and protic organic solvents as well as in aqueous solution.

Foldamers

L. Mathieu, B. Legrand, C. Deng,
L. Vezenkov, E. Wenger, C. Didierjean,
M. Amblard, M.-C. Averlant-Petit,
N. Masurier, V. Lisowski, J. Martinez,
L. T. Maillard* ______ **6006 – 6010**

Helical Oligomers of Thiazole-Based γ-Amino Acids: Synthesis and Structural Studies

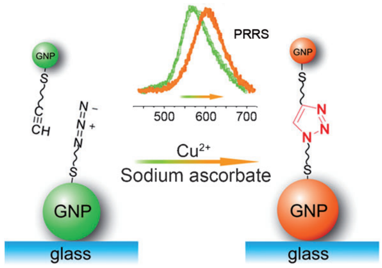

A method based on plasmon resonance Rayleigh scattering (PRRS) spectroscopy and dark-field microscopy (DFM) was established for the real-time monitoring of a click reaction at the single-nanoparticle level. Click reactions on the surface of single gold nanoparticles (GNPs) result in interparticle coupling, which leads to a red-shift of the λ_{max} ($\Delta\lambda_{max} = 43$ nm) in the PRRS spectra and a color change of the single gold nanoparticles in DFM (from green to orange).

Click Chemistry

L. Shi, C. Jing, W. Ma, D.-W. Li, J. E. Halls,
F. Marken, Y.-T. Long* ______ **6011 – 6014**

Plasmon Resonance Scattering Spectroscopy at the Single-Nanoparticle Level: Real-Time Monitoring of a Click Reaction

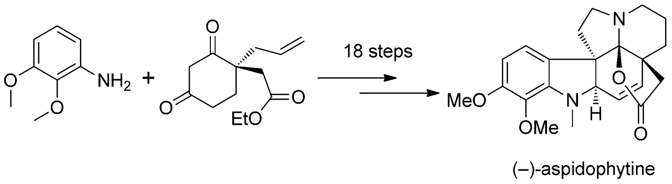

A general approach toward the asymmetric total synthesis of various aspidosperma alkaloids includes the combination of a C–H bond activation with a Heck-type coupling, and the stereocontrolled formation of piperidine and pyrrolidine rings as key steps. The feasibility of this approach was demonstrated with the total synthesis of aspidophytine in 18 steps from 4,4-disubstituted cyclohexanedione and 2,3-dimethoxyaniline (see scheme).

Total Synthesis

R. Yang, F. G. Qiu* ______ **6015 – 6018**

General Entry to Aspidosperma Alkaloids: Enantioselective Total Synthesis of (−)-Aspidophytine

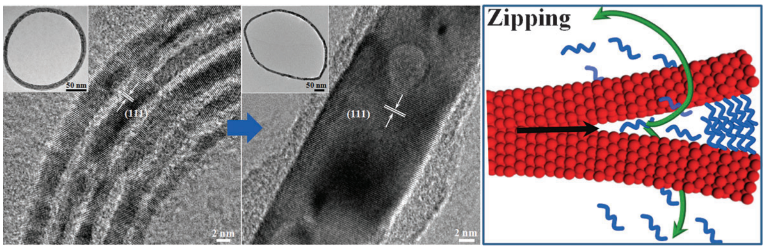

Parallel-stacked gold nanowires (NWs) in a ring conformation are induced to coalesce, forming solid seamless rings. The axial lattice orientation of the original Au NWs is preserved in the coalesced rings (see picture; scale bars 2 nm, insets 50 nm). A zipper mechanism is proposed to reconcile the three major events in coalescing nanocrystals: ligand loss, lattice alignment, and coalescence.

Crystal Coalescence

J. Xu, Y. Wang, X. Qi, C. Liu, J. He,
H. Zhang, H. Chen* ______ **6019 – 6023**

Preservation of Lattice Orientation in Coalescing Imperfectly Aligned Gold Nanowires by a Zipper Mechanism

Fluorinated Compounds

An efficient protocol for the selective fluorination of benzylic C–H bonds is described. The process is catalyzed by manganese salen complexes and uses nucleophilic fluorine sources, such as triethylamine trihydrofluoride and KF. Reaction rates are sufficiently high (30 min) to allow adoption for the incorporation of ^{18}F fluoride sources for PET imaging applications.

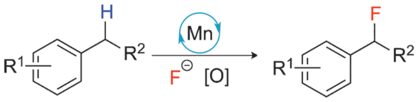

Nanomaterials

Inside Cover

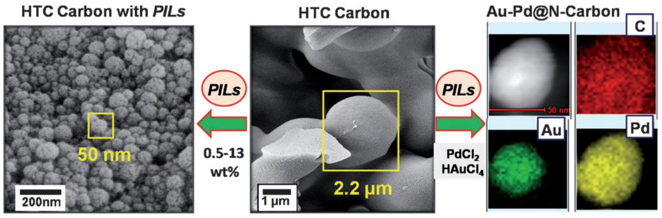

Pores for thought: Porous nitrogen-doped carbon materials (HTC Carbon with PILs) composed of spherical nanoparticles, and also those with Au–Pd core–shell nanoparticles embedded (Au–Pd@N-Carbon) were synthesized. These materials can be prepared from sugars by hydrothermal carbonization (160–200 °C) in the presence of poly(ionic liquid)s (PILs), which act as a stabilizer, pore-generating agent, and nitrogen source.

Synthetic Methods

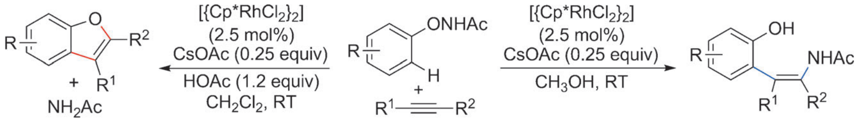

Give it a tweak: A novel oxidizing directing group was developed for a rhodium(III)-catalyzed C–H functionalization of *N*-phenoxyacetamides with alkynes. A small change in the reaction conditions leads to either *ortho*-hydroxyphenyl-substituted enamides or cyclization to deliver benzofurans with high selectivity (see scheme; Cp* = C_5Me_5).

Cascade Reactions

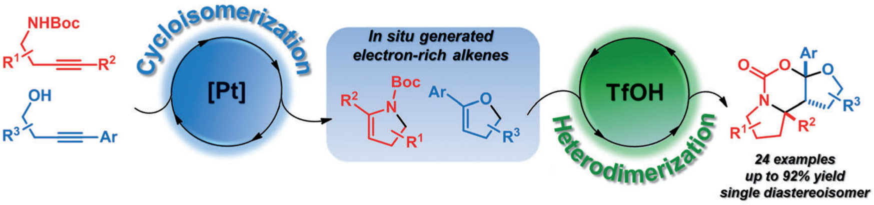

Complex heterocyclic products were synthesized from simple alkynamine and alkynol derivatives in a double cycloisomerization/heterodimerization cascade reaction (see scheme). The reaction includes the heterocoupling reaction of two different electron-rich alkenes and leads to the formation of four new bonds and three stereocenters (two of them quaternary).

Direct Amination

L. D. Tran, J. Roane, O. Daugulis* ———— **6043 – 6046**

Directed Amination of Non-Acidic Arene C−H Bonds by a Copper–Silver Catalytic System

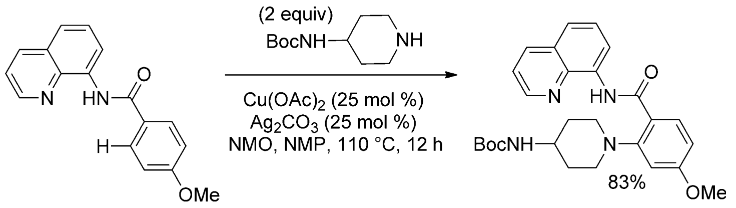

Amine meets arene: A method for direct amination of β-C(sp^2)−H bonds of benzoic acid derivatives and γ-C(sp^2)−H bonds of benzylamine derivatives has been developed. The reaction is catalyzed by Cu(OAc)$_2$ and a Ag$_2$CO$_3$ cocatalyst, and shows high generality and functional-group tolerance, as well as providing a straightforward means for the preparation of *ortho*-aminobenzoic acid derivatives.

Crystal Structure Analysis

M. Müller, C. M. Orben, N. Schützenmeister, M. Schmidt, A. Leonov, U. M. Reinscheid,* B. Dittrich,* C. Griesinger * **6047 – 6049**

The Absolute Configuration of (+)- and (−)-*erythro*-Mefloquine

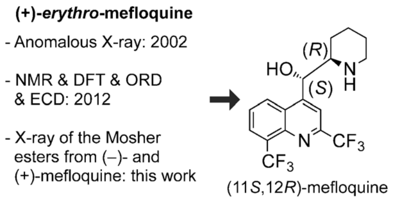

The controversy over the absolute configuration of (+)-*erythro*-mefloquine, the less psychosis-causing enantiomer of the antimalarial drug Lariam, has been resolved by Mosher ester crystallization. The configuration determined previously by physical methods (see scheme) is correct, whereas the configuration determined by three enantioselective syntheses is wrong.

Asymmetric Catalysis

G. Ma, S. Afewerki, L. Deiana, C. Palo-Nieto, L. Liu, J. Sun, I. Ibrahem,* A. Córdova* ———— **6050 – 6054**

A Palladium/Chiral Amine Co-catalyzed Enantioselective Dynamic Cascade Reaction: Synthesis of Polysubstituted Carbocycles with a Quaternary Carbon Stereocenter

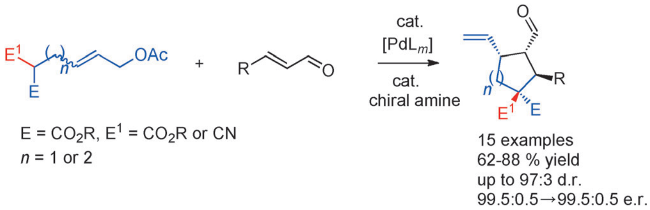

Polysubstituted 5- and 6-membered carbocycles were synthesized by the title reaction. The one-pot dynamic relay process generates four new stereocenters, including a quaternary carbon center, in a highly enantioselective fashion (99.5:0.5→99:0.5 e.r.) by using a simple combination of palladium and chiral amine co-catalysts.

Aptamer Microarray

X. Zhang, S. Zhu, Y. Xiong, C. Deng,* X. Zhang* ———— **6055 – 6058**

Development of a MALDI-TOF MS Strategy for the High-Throughput Analysis of Biomarkers: On-Target Aptamer Immobilization and Laser-Accelerated Proteolysis

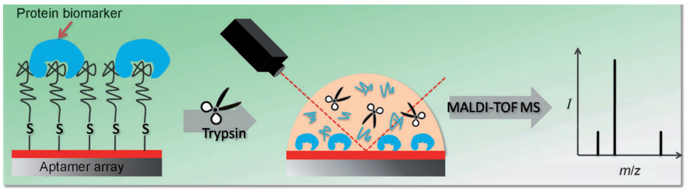

An aptamer-based strategy was developed for the high-throughput analysis of protein biomarkers, such as lysozyme, by on-target MALDI-TOF MS. The aptamers were immobilized on the target plate through formation of covalent bonds with a stable and porous gold layer. An infrared laser was subsequently applied for fast proteolysis (see picture). High sensitivities were observed both in standard solutions and human urine.

Bioinorganic Chemistry

E. Wexselblatt, E. Yavin,
D. Gibson* ________ 6059 – 6062

Platinum(IV) Prodrugs with Haloacetato Ligands in the Axial Positions can Undergo Hydrolysis under Biologically Relevant Conditions

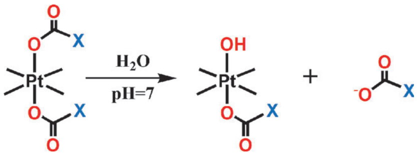

Losing ligands rapidly: Pt^{IV} complexes with haloacetato ligands can hydrolyze rapidly under biological conditions (pH 7 and 37 °C, see scheme) and the rate increases with increasing pH value. Possible mechanisms for this hydrolysis are examined using $H_2{}^{18}O$ and ESI-MS analysis.

Nanostructures

X. Huang, Y. Li, Y. Chen, H. Zhou, X. Duan,
Y. Huang* ________ 6063 – 6067

Plasmonic and Catalytic AuPd Nanowheels for the Efficient Conversion of Light into Chemical Energy

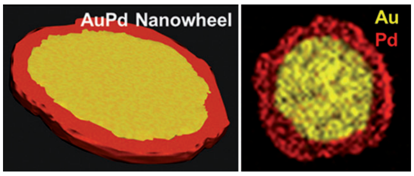

Reinventing the wheel: Bimetallic AuPd nanowheels (see picture), a freestanding form of 2D AuPd nanostructures, were synthesized in a one-pot process. The well-defined and tunable surface plasmon resonance displayed by these nanowheels was exploited in a unique catalytic process in which light energy was used to drive catalytic reactions, such as the Suzuki coupling, with much higher efficiency than that of the conventional heating process.

Glycosylation

J. Zheng, K. B. Urkalan,
S. B. Herzon* ________ 6068 – 6071

Direct Synthesis of β-*N*-Glycosides by the Reductive Glycosylation of Azides with Protected and Native Carbohydrate Donors

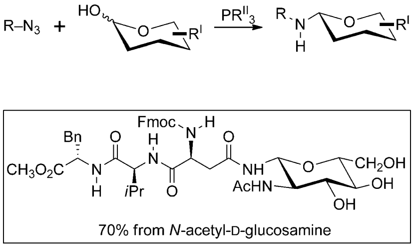

A simple and straightforward method for the stereocontrolled synthesis of β-linked *N*-glycosides uses alkyl and aryl azides as the nitrogen source. The *N*-glycosides are formed in high yields and with high β selectivities (typically > 70% yield, > 15:1 β:α selectivity). This approach is also amenable to the synthesis of *N*-glycosylated amino acids and peptides (see example, Fmoc = 9-fluorenylmethoxycarbonyl).

Synthetic Methods

S. Song, S.-F. Zhu, L.-Y. Pu,
Q.-L. Zhou* ________ 6072 – 6075

Iridium-Catalyzed Enantioselective Hydrogenation of Unsaturated Heterocyclic Acids

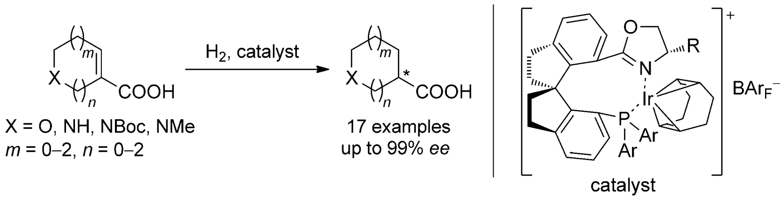

Spiral binding: A highly enantioselective hydrogenation of unsaturated heterocyclic acids has been developed by using chiral iridium/spirophosphino oxazoline catalysts (see scheme; $BAr_F^- =$ tetrakis[3,5-bis(trifluoromethyl)phenyl]borate, Boc = *tert*-butoxycarbonyl). This reaction provided an efficient method for the preparation of optically active heterocyclic acids with excellent enantioselectivities.

Polycyclic Hydrocarbons

A. Shimizu, R. Kishi, M. Nakano, D. Shiomi, K. Sato, T. Takui, I. Hisaki, M. Miyata, Y. Tobe* ———— **6076 – 6079**

Indeno[2,1-*b*]fluorene: A 20-π-Electron Hydrocarbon with Very Low-Energy Light Absorption

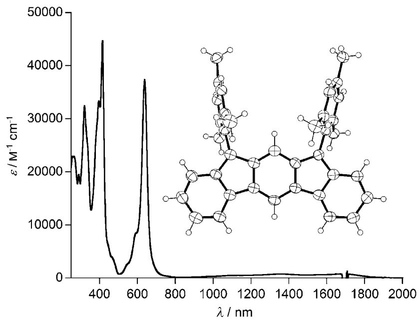

Smaller can be better: The first example of *meta*-quinodimethane embedded in an indenofluorene framework has been synthesized. 10,12-Dimesitylindeno[2,1-*b*]fluorene exhibits extremely low-energy light absorption, despite the small conjugation space of the molecule, which consists of only 20 π electrons.

Back Cover

Pyrrole Alkylation

L. Jiao, T. Bach* ———— **6080 – 6083**

Palladium-Catalyzed Direct C–H Alkylation of Electron-Deficient Pyrrole Derivatives

The apparent and the real: What looks like a Friedel–Crafts alkylation reaction of electron-deficient pyrroles is actually a Pd^{II}-catalyzed, norbornene-mediated C–H activation reaction, in which the alkylation of the pyrrole core occurs by reductive elimination. As well as ethyl-1*H*-pyrrole-2-carboxylate (see scheme), several other 2,3-disubstituted pyrroles underwent the selective C5 alkylation in good yield.

Carbohydrate Biosensors

D. Pussak, D. Ponader, S. Mosca, S. V. Ruiz, L. Hartmann,* S. Schmidt* ———— **6084 – 6087**

Mechanical Carbohydrate Sensors Based on Soft Hydrogel Particles

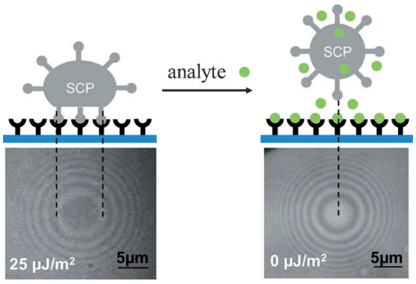

Elastic sensors: A simple method is presented for the measurement of specific biomolecular interactions with soft colloidal hydrogel particles (SCPs) as sensors. Carbohydrate/lectin interactions (see picture; green: carbohydrate molecules) were studied by optical detection of the mechanical deformation of the particles on a lectin surface. The affinity of various carbohydrate inhibitors could also be readily determined.

Nanomaterials

F. Böttger-Hiller, P. Kempe, G. Cox, A. Panchenko, N. Janssen, A. Petzold, T. Thurn-Albrecht, L. Borchardt, M. Rose, S. Kaskel, C. Georgi, H. Lang, S. Spange* ———— **6088 – 6091**

Twin Polymerization at Spherical Hard Templates: An Approach to Size-Adjustable Carbon Hollow Spheres with Micro- or Mesoporous Shells

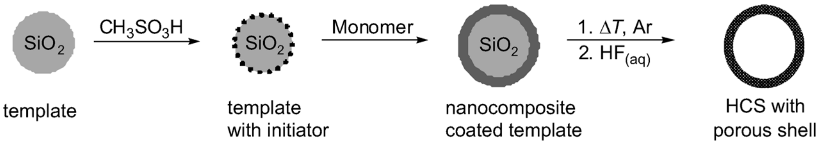

Kitset hollow spheres: The combination of twin polymerization with hard templates makes hollow carbon spheres (HCSs) with tailored properties easily accessible. The thickness and pore texture of the HCS shells and also the diameter of the spherical cavity can be varied. The application potential of synthesized HCS is substantiated by an excellent cycling stability of lithium–sulfur batteries.

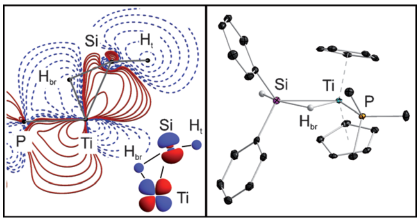

Experimental and theoretical charge density studies and molecular orbital analyses suggest that the complexes [$Cp_2Ti(PMe_3)SiH_2Ph_2$] (**1**) and [$Cp_2Ti(PMe_3)SiHCl_3$] (**2**) display virtually the same electronic structures. No evidence for a significant interligand hypervalent interaction could be identified for **2**. A bonding concept for transition-metal hydrosilane complexes aims to identify the true key parameters for a selective activation of the individual M−Si and Si−H bonds.

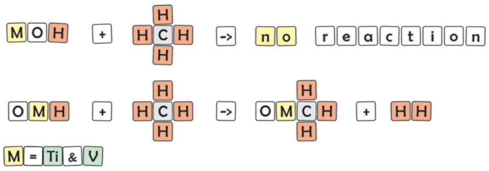

Methane scrabble: To have the right elements is sometimes just not sufficient, as shown by [M(OH)]$^+$ (M = Ti, V), which do not react with methane. However, reshuffling of the "tiles" to [HMO]$^+$ changes the reactions behavior completely, leading to the first example of C−H bond activation of methane by an early first-row transition-metal cation.

DOI: 10.1002/anie.201303275

50 Years Ago . . .

Angewandte Chemie International Edition was first published in 1962, the mother journal first in 1888. In this monthly flashback, we feature some of the articles that appeared 50 years ago. This look back can open our eyes, stimulate discussion, or even raise a smile.

Promethium was first produced at Oak Ridge National Laboratory in 1945, but it was only in 1963 that metallic promethium was isolated. F. Weigel reported in a Communication how a sample of processed promethium (which contained other lanthanoid isotopes) from Oak Ridge was purified by ion-exchange chromatography and used to prepare promethium trifluoride, which was then heated under high vacuum to produce metallic promethium.

Hubert Schmidbaur and Hermann Hussek outlined the synthesis of lithium trimethylstannolate ($LiOSn(CH_3)_3$) in a Communication. The target compound was prepared by reaction of hexamethyldistannoxane with methyllithium, and could be used to prepare alkyl(di)stannosiloxanes. Schmidbaur was previously Chairman of the Editorial Board of *Angewandte Chemie* and his Essay on coordination chemistry at carbon was published in our recent Jubilee Issue celebrating 125 years of *Angewandte Chemie* (*Angew. Chem. Int. Ed.* **2013**, 176–186).

The Mössbauer Effect was discovered in 1958, and its origins and applications were discussed in a Review by E. Fluck et al. Compounds that had been investigated by using Mössbauer spectroscopy included potassium ferrates, iron carbonyls, and Prussian Blue.

Read more in Issue 6/1963

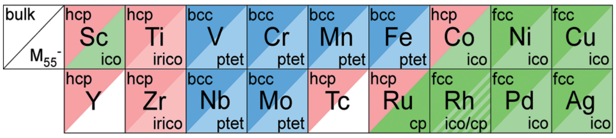

bulk / M_{55}^-	Sc	Ti	V	Cr	Mn	Fe	Co	Ni	Cu
bulk	hcp	hcp	bcc	bcc	bcc	bcc	hcp	fcc	fcc
M_{55}^-	ico	irico	ptet	ptet	ptet	ptet	ico	ico	ico

bulk / M_{55}^-	Y	Zr	Nb	Mo	Tc	Ru	Rh	Pd	Ag
bulk	hcp	hcp	bcc	bcc	hcp	hcp	fcc	fcc	fcc
M_{55}^-		irico	ptet	ptet		cp	ico/cp	ico	ico

Correlation of cluster and bulk structure: Electron-diffraction measurements of homonuclear 55-atom transition-metal cluster anions covering essentially all 3d and 4d elements show only four main structure families. Elements with the same bulk lattice morphology generally have a common cluster structure type. The cluster structure types differ in maximum atomic coordination numbers in analogy to the coordination numbers in the corresponding bulk lattices.

Cluster Structures

T. Rapps, R. Ahlrichs, E. Waldt,
M. M. Kappes, D. Schooss* **6102 – 6105**

On the Structures of 55-Atom Transition-Metal Clusters and Their Relationship to the Crystalline Bulk

Inside Back Cover

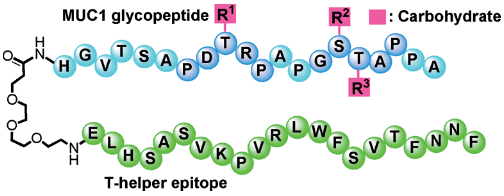

The T-helper epitope peptide P30 (green in the scheme) from tetanus toxoid was used as the immunostimulant in MUC1 glycopeptide antitumor vaccines and apparently also acts as a built-in adjuvant. P30-conjugated glycopeptide vaccines containing three glycans in the immunodominant motifs PDTRP and GSTAP induced much stronger immune responses and complement dependent cytotoxicity mediated killing of tumor cells when applied in plain PBS solution without complete Freund's adjuvant.

Antitumor Vaccines

H. Cai, M.-S. Chen, Z.-Y. Sun, Y.-F. Zhao,
H. Kunz,* Y.-M. Li* ——— **6106 – 6110**

Self-Adjuvanting Synthetic Antitumor Vaccines from MUC1 Glycopeptides Conjugated to T-Cell Epitopes from Tetanus Toxoid

---

Supporting information is available on www.angewandte.org (see article for access details).

A video clip is available as Supporting Information on www.angewandte.org (see article for access details).

This article is available online free of charge (Open Access).

This article is accompanied by a cover picture (front or back cover, and inside or outside).